

Mitigating thermal runaway of lithium-ion battery through electrolyte displacement

Yang Shi, Daniel J. Noelle, Meng Wang, Anh V. Le, Hyojung Yoon, Minghao Zhang, Ying Shirley Meng, Jiang Fan, Dengguo Wu, and Yu Qiao

Citation: *Appl. Phys. Lett.* **110**, 063902 (2017); doi: 10.1063/1.4975653

View online: <http://dx.doi.org/10.1063/1.4975653>

View Table of Contents: <http://aip.scitation.org/toc/apl/110/6>

Published by the [American Institute of Physics](#)



**FIND THE NEEDLE IN THE
HIRING HAYSTACK**

POST JOBS AND REACH THOUSANDS OF
QUALIFIED SCIENTISTS EACH MONTH.

PHYSICS TODAY | JOBS
WWW.PHYSICSTODAY.ORG/JOBS

Mitigating thermal runaway of lithium-ion battery through electrolyte displacement

Yang Shi,¹ Daniel J. Noelle,¹ Meng Wang,² Anh V. Le,² Hyojung Yoon,³ Minghao Zhang,³ Ying Shirley Meng,³ Jiang Fan,⁴ Dengguo Wu,⁴ and Yu Qiao^{1,2,a)}

¹Program of Materials Science and Engineering, University of California – San Diego, La Jolla, California 92093, USA

²Department of Structural Engineering, University of California – San Diego, La Jolla, California 92093-0085, USA

³Department of Nanoengineering, University of California – San Diego, La Jolla, California 92093, USA

⁴American Lithium Energy Corporation, 1485 Poinsettia Ave., Vista, California 92081, USA

(Received 9 November 2016; accepted 17 January 2017; published online 6 February 2017)

Alkanes are investigated as thermal-runaway retardants (TRR) for lithium-ion battery (LIB). TRR is a chemical that can rapidly terminate exothermic reactions in LIB. Under normal working conditions, TRR is sealed in separate packages in the LIB cell, and upon mechanical abuse, it is released to suppress heat generation. The alkanes under investigation include octane, pentadecane, and icosane, among which pentadecane has the highest thermal-runaway mitigation (TRM) efficiency. In nail penetration test on coin cells, ~4 wt. % pentadecane reduced the maximum temperature by ~60%; in impact test on pouch cells, ~5 wt. % pentadecane reduced the maximum temperature by ~90%. The high TRM efficiency of pentadecane is attributed to its high wettability to separator and its immiscibility with electrolyte. By forming a physical barrier between the cathode and anode, pentadecane interrupts lithium ion (Li^+) transport and increases the charge transfer resistance by nearly two orders of magnitude. The diffusion rate of pentadecane in the electrode layer stack was measured to be ~580 $\mu\text{m/s}$. *Published by AIP Publishing.* [<http://dx.doi.org/10.1063/1.4975653>]

Tremendous progress was achieved in the last few decades on the development of lithium-ion battery (LIB). In terms of specific cost and energy density, LIBs by far outperform lead acid batteries, nickel metal hydride batteries, and supercapacitors, and have been widely employed in commercial and military fields.¹ Recently, intensive research is being conducted to extend the application of LIB to large-scale energy storage systems, such as electric vehicles with drive range more than 300 miles² and smart grids on the scale of 0.6–4.3 MW.³ As the battery structure is scaled up, the system damage tolerance becomes a “bottleneck.”

Under normal working conditions, the cathode and the anode in a LIB are separated by a thin porous membrane, which can be ruptured if the battery is mechanically abused. Under this condition, the cathode and the anode are in direct contact, creating internal shorting sites (ISS) surrounding the damaged areas. The large amount of stored energy is rapidly dissipated in the ISS, resulting in a high increase in temperature. When the temperature rises to above 90 °C, a series of exothermic electrochemical reactions and chemical decompositions takes place, and thermal runaway occurs.⁴ Battery fire hazard imposes a tough challenge to the safety and robustness of LIB-based energy storage devices.

A promising approach to mitigate thermal runaway is to shut down the reactions when the LIB cell malfunctions. For the most adverse conditions, the shutdown mechanism must be spontaneous, independent of external control modules or integrated electronic elements. Positive-temperature-coefficient (PTC) materials may be coated on current collectors, which increases the internal impedance at 90–130 °C.^{5–7}

Microspheres or layers of melting points around 110 °C are incorporated in anodes or separators, which could melt and block ion transport.^{8,9} However, thermal runaway has already begun at such temperatures. The shutdown processes of PTC additives or low-melting-point materials have to compete against the fast and intense local heat generation.

It is desirable that the thermal-runaway mitigation (TRM) mechanism can be activated immediately after the battery is damaged, even before the temperature begins to increase. Recently, we investigated mechanically triggered TRM approaches.^{10–13} When the cell was mechanically abused, a thermal-runaway retardant (TRR) was released into the battery cell to significantly reduce the heat generation rate. The amount of TRR was less than 5%, so that the reduction in effective specific energy was trivial. Under normal conditions, TRR was sealed in separate packages neutral to the battery environment. Experimental data showed that polyethylene-based multilayer TRR packages had little influence on the electrochemical performance of LIB cells.¹⁴

In our previous work, we studied aliphatic amines as TRR.^{14,15} One promising TRM mechanism is electrolyte displacement: If the TRR is more wettable to electrodes or separator than the electrolyte, it may form a thin layer that blocks lithium ion (Li^+) transport. In the current study, a class of low-toxic chemicals, alkanes, are examined as TRR candidates. We focus on octane, pentadecane, and icosane, representing alkanes of low, intermediate, and high molecular weights, respectively.

Nail penetration tests on coin cells were performed through the same procedure as in Ref. 14. Fully charged (4.3 V) LIR-2450 cells were disassembled and re-assembled in modified cell cases with two holes, which allowed for the

^{a)}Email: yqiao@ucsd.edu. Telephone: +1-858-534-3388.

injection of TRR. Immediately prior to the nail penetration, 100 μL octane, pentadecane, or pristine electrolyte (1 M LiPF_6 in EC:EMC wt 1:1) were injected into the modified cell. Icosane was solid at room temperature. To test its influence on heat generation of damaged LIB cells, 0.1 g icosane was grounded into powders and placed next to the electrodes inside re-assembled cell before nail penetration. The temperature of the cells was recorded by a thermal couple attached to the cell case.

Wettability tests and contact angle measurements (KSV Instruments CAM 100) were carried out by dropping 50 μL electrolyte or pentadecane on Celgard 2320 separators.

To evaluate the influence of pentadecane on cell resistance, coin cells were assembled with cathode films composed of $\text{LiNi}_{0.5}\text{Co}_{0.2}\text{Mn}_{0.3}\text{O}_2$, polyvinylidene fluoride, and carbon black, with the mass ratio of 93:4:3; lithium metal served as the anode. Extra pentadecane was added into the cell; the mass of pentadecane was 4% of the total mass of electrodes, separator, and electrolyte. Reference coin cells were assembled without pentadecane. Electrochemical impedance spectroscopy (EIS) measurements were carried out at room temperature on the reference and the pentadecane-modified cells, in the frequency range of 10^6 Hz to 10^{-2} Hz with the signal amplitude of 10 mV.

Diffusion rate measurement was performed. Double-side coated cathode (MTI, bc-af-241NCM-523) and anode (MTI, bc-cf-241-ds) sheets as well as separators (Celgard 2320) were punched into disks with diameters of 63.5 mm. Three layers of cathode, three layers of anode, and six layers of separators were stacked alternately to form an electrode stack. A 3-mm-diameter hole was punched through the center of the stack. A mold made of poly(methyl methacrylate) with built-in channels for pentadecane insertion was placed on top of the electrode stack, and they were sandwiched in between two compression plates of a type-5582 Instron machine, with the compression pressure of 1 kPa. 200 μL pentadecane was inserted through the built-in channel, and the diffusion distances were measured after 15 s, 30 s, and 45 s.

Pouch cells embedded with TRR packages were assembled to evaluate the efficiency of TRR in large-sized LIB. PAP trilayer sheet (ULINE S-16893) was folded and heat sealed to form cylindrical packages using an impulse sealer (McMaster-Carr). A gelatin straw was inserted into the PAP cylinder as the scaffold, and pentadecane was injected. The final cylindrical package had the diameter of ~ 6 mm and the length of ~ 35 mm. Four packages were embedded in one pouch cell. The mass percentage of the TRR packages was 5% of the pouch cell. Double-side coated cathode (MTI, bc-af-241NCM-523) and anode (MTI, bc-cf-241-ds) were cut into rectangular sheets with the length of ~ 60 mm and the width of ~ 47 mm. The electrode sheets were modified by creating four openings. The pouch cells were assembled with 11 layers and 12 layers of modified cathode and anode sheets, respectively, embedded with empty or TRR packages. UL 1642 standard impact test was performed on the pouch cells. A stainless steel rod with the diameter of 16 mm and the length of 66.5 mm was affixed at the upper surface of the pouch cell. A 9-kg hammer was dropped from a distance

of 0.6 m. The temperature of the cell was recorded by a thermocouple affixed at the cell surface.

In the nail penetration test, TRR is injected into the testing cell immediately before the nail penetration takes place.¹⁴ Three straight-chain alkanes, namely, octane, pentadecane, and icosane, are tested. Figure 1(a) shows the temperature profiles of the cells after nail penetration. All alkanes lead to reduced peak temperature increase (ΔT_{max}) while pentadecane results in the smallest ΔT_{max} . The addition of pentadecane reduces ΔT_{max} by $\sim 60\%$, from $\sim 75^\circ\text{C}$ in the reference cell to $\sim 30^\circ\text{C}$. Figure 1(b) shows the calculated heat generation for the first 20 minutes after nail penetration, using the heat transfer model developed in Ref. 14. The addition of 4 wt. % pentadecane leads to $\sim 50\%$ reduction in heat generation, from ~ 0.23 Wh in reference cell to ~ 0.12 Wh. Octane has a lower efficiency, possibly due to its low boiling point $\sim 125^\circ\text{C}$. After nail penetration, the temperature inside the LIB cell increases rapidly and causes evaporation of octane. Icosane has a melting point of 36°C and would be melted inside the cell after nail penetration. It could flow and wet the separator after melting, but with a higher viscosity and a shorter diffusion distance. That is, the optimum alkane TRR should have an intermediate chain length, such as pentadecane.

To investigate the TRM mechanism of pentadecane, wettability and contact angle tests are performed, as shown in Fig. 2(a). It is evident that pentadecane could spread over a

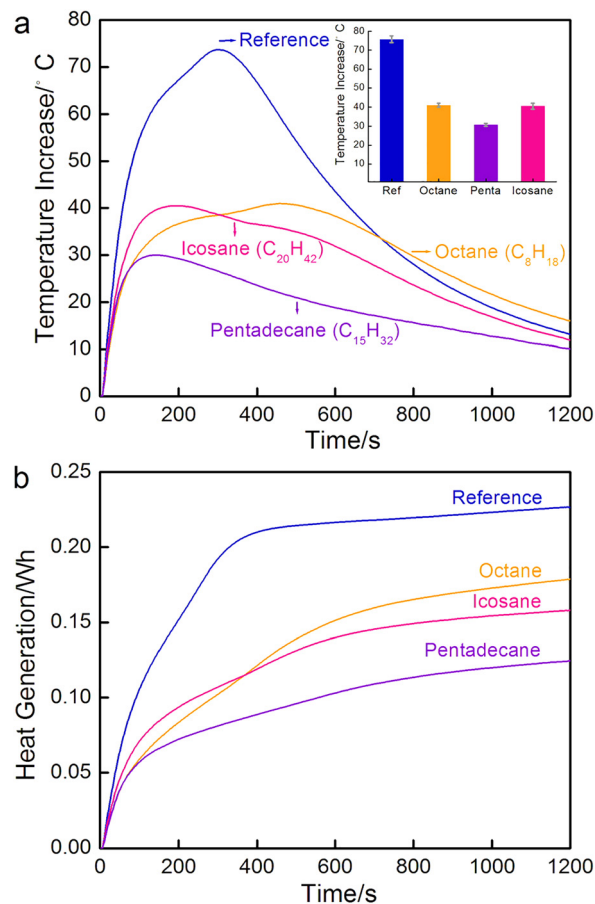


FIG. 1. (a) Typical temperature profiles measured in nail penetration tests on reference and alkanes-modified coin cells; the inset shows the peak temperature increase with error bars. (b) Calculated heat generation of reference and alkanes-modified cells.

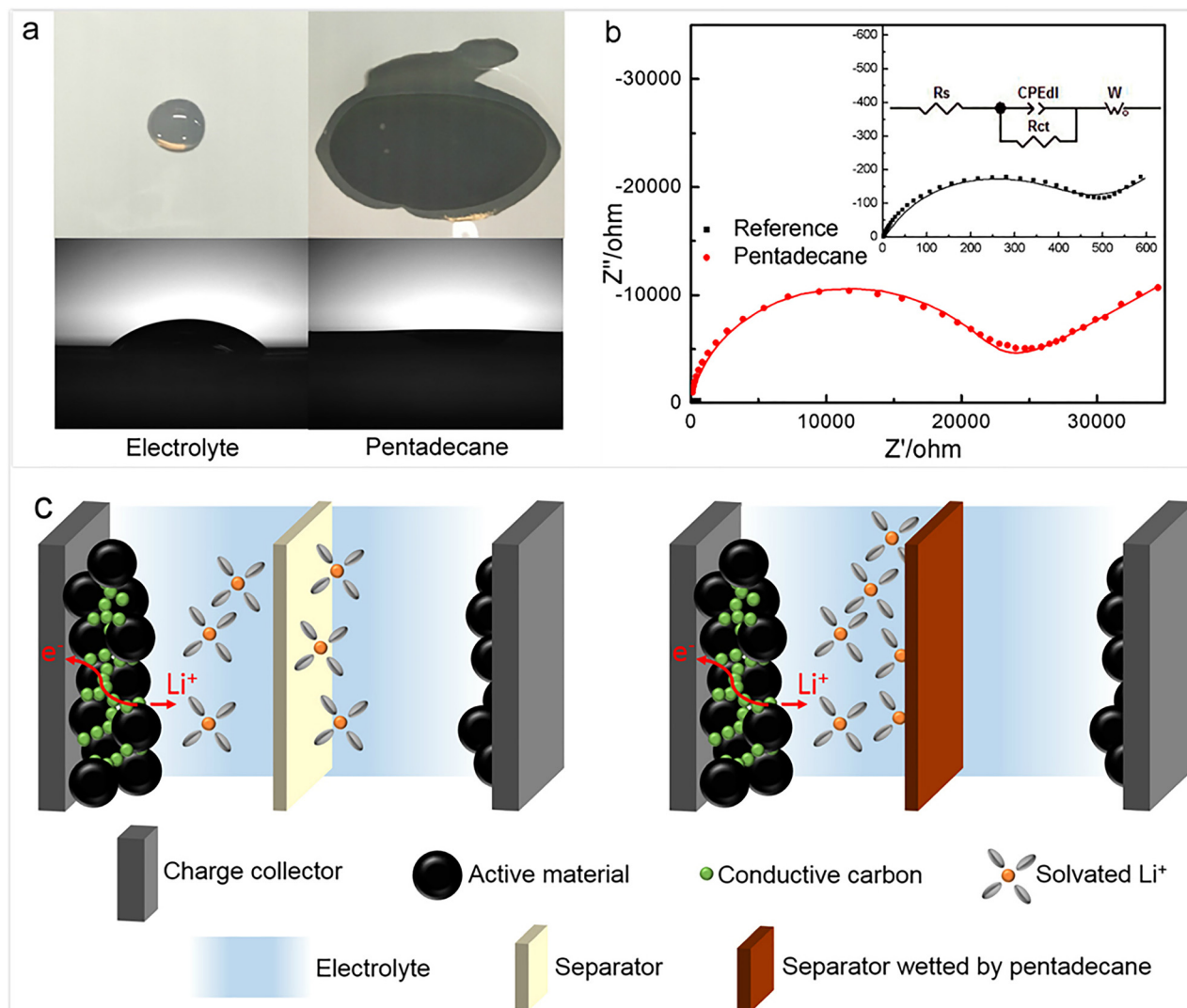


FIG. 2. (a) Diffusion tests (above) and contact angle measurement (below) of electrolyte and pentadecane; the photos were taken after the liquid was dropped on the substrate for 15 s. (b) Nyquist plots, equivalent circuits, and fitting plots of reference and pentadecane-modified coin cells. (c) Illustration of the working mechanism of pentadecane.

much larger area on the separator than electrolyte. The contact angle measurement confirms that pentadecane is much more wettable to the separator. Since pentadecane is immiscible with the electrolyte and is more wettable to the separator, it will repel electrolyte and form a physical blocking layer in the separator, which suppresses Li^+ transport. According to the EIS fitted results in Fig. 2(b), the series resistance (R_s) for reference and pentadecane-modified cells are 1.72Ω and 85.1Ω , respectively; the charge transfer resistance (R_{ct}) for reference and pentadecane-modified cells are 375.2Ω and 20004.3Ω , respectively. Both R_s and R_{ct} increase by ~ 50 times with the addition of pentadecane. Figure 2(c) illustrates the working mechanism of pentadecane. The charge transfer reactions at the electrode-electrolyte interface are suppressed due to the accumulation of reaction products (Li^+).

The diffusion rate of pentadecane in electrode layers is a key parameter.¹⁶ The diffusion rate measurement setup is illustrated in Fig. 3(a). Longitudinal wicking from the central reservoir occurs when the liquid wets the porous structure.¹⁷ The diffusion distance, l , of a liquid flowing under capillary pressure is given by the Washburn-Lucas equation¹⁸

$$l^2 = \left(\frac{\gamma \cos \theta}{\eta} \right) rt, \quad (1)$$

where γ is the liquid surface tension, η is the liquid viscosity, θ is the contact angle, r is the effective capillary radius, and t is time. It shows a linear relationship between t and l^2 , fitting well with Fig. 3(b). The surface tension and the viscosity of pentadecane are 25.8 mN/m and 2.841 cP , respectively.¹⁹ The contact angle of pentadecane on separators and electrodes are 0° . Figure 3(c) shows cathode, anode, and separator after diffusion tests. The wetted areas are circular or elliptical. The diffusion distance is defined as the radius of circle or the average of semi-major and semi-minor axes of ellipse. The calculated effective capillary radii are $33.1 \mu\text{m}$, $31.6 \mu\text{m}$, and $22.7 \mu\text{m}$ for anode, cathode, and separator, respectively. When the electrode stack is compressed at 1 kPa , pentadecane could travel 8.7 mm on separator in 15 s . Such a measurement is conservative, since in a LIB cell, nail penetration or impact would damage local electrodes, leading to a loosely packed structure that favors capillary flow.

In order to incorporate TRR into a large-sized pouch cell, the electrodes are modified to host TRR packages. The

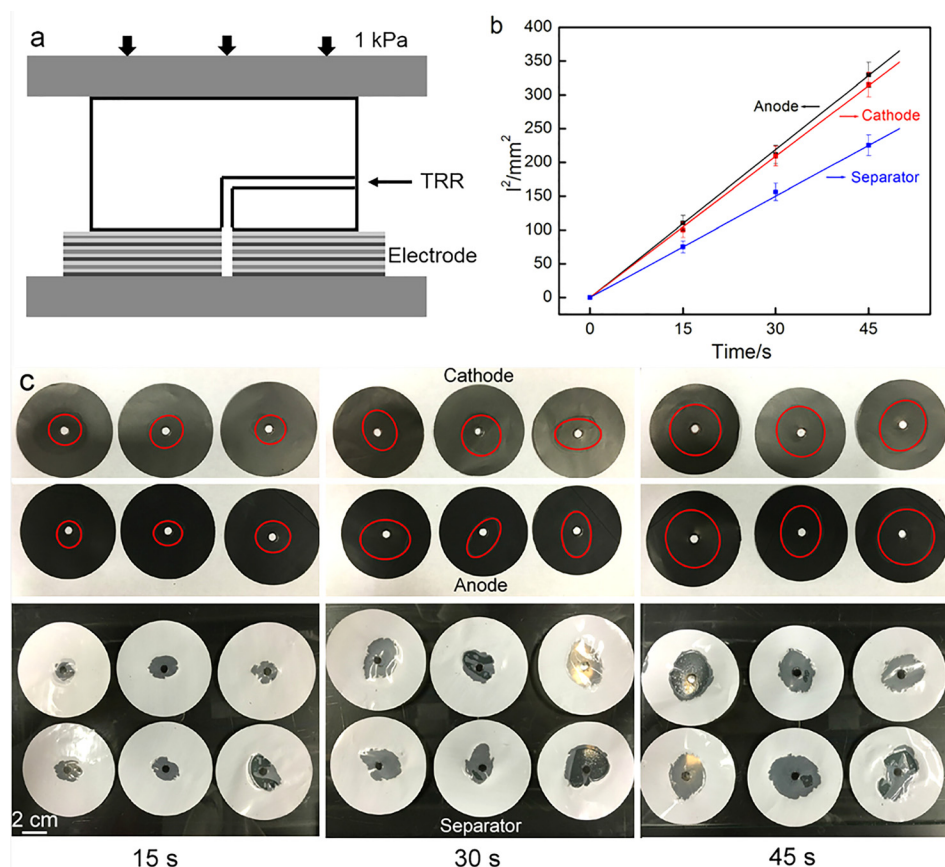


FIG. 3. (a) Schematic of the diffusion rate measurement setup. (b) The relationship between the diffusion distance (l) and time (t). (c) Typical photos of cathode, anode, and separator in the diffusion rate measurement experiment.

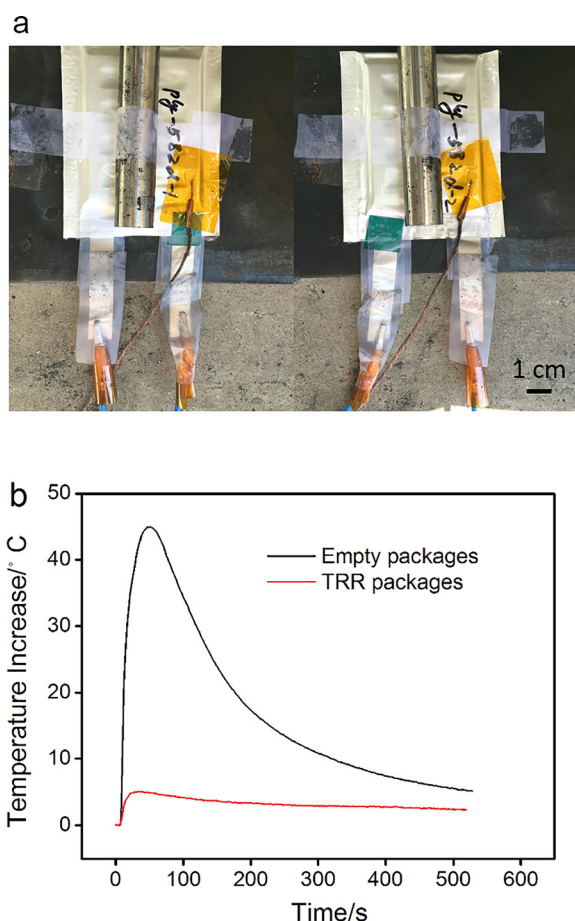


FIG. 4. (a) Pouch cells embedded with empty packages and TRR packages. (b) Temperature profiles of pouch cells in impact test.

pouch cells under investigation are shown in Fig. 4(a) and described in Table I. The reference cell and the TRR-modified cell have similar capacity and impedance values. Upon impact, the temperature profiles of reference and TRR-modified pouch cells are shown in Fig. 4(b). The maximum increase in temperature of the pouch cell embedded with TRR is only 5 °C, order-of-magnitude lower than that of the reference cell. The temperature ramping rate of the reference cell and the TRR-containing cell are similar in the first few seconds. After that, the temperature of TRR-containing cell rises much more slowly than the reference cell, suggesting that TRR takes effect shortly after the package is broken apart. The sudden breakage of TRR packages favors TRR delivery.

In summary, pentadecane is identified as an efficient and low-toxic thermal-runaway retardant (TRR) of lithium-ion battery (LIB). In the nail penetration test of coin cells, 4 wt. % pentadecane reduces the peak temperature increase by ~60%, better than octane and icosane; in impact test of pouch cells, 5 wt. % pentadecane reduces the peak temperature increase by nearly an order of magnitude. The working mechanism of pentadecane is associated with its superior wettability to the separator material. Through electrolyte displacement, Li^+ transport is suppressed; with 4 wt. % pentadecane, series resistance and charge transfer resistance are

TABLE I. Parameters of LIB pouch cells.

	Capacity	Voltage	Cell mass	Impedance
Reference cell	0.754 Ah	4.20 V	20.0 g	19.58 mΩ
Modified cell	0.706 Ah	4.20 V	21.0 g	19.78 mΩ

increased by ~ 50 times. The diffusion rate measurement demonstrates that pentadecane can travel ~ 8.7 mm in 15 s in an electrode layer stack.

This research was supported by Advanced Research Projects Agency - Energy (ARPA-E) under Grant No. DE-AR0000396, for which we are grateful to Dr. Ping Liu, Dr. John Lemmon, Dr. Grigori Soloveichik, Dr. Chris Atkinson, and Dr. Dawson Cagle.

- ¹V. Etacheri, R. Marom, R. Elazari, G. Salitra, and D. Aurbach, "Challenges in the development of advanced Li-ion batteries: a review," *Energy Environ. Sci.* **4**, 3243 (2011).
- ²M. M. Thackeray, C. Wolverton, and E. D. Isaacs, "Electrical energy storage for transportation—approaching the limits of, and going beyond, lithium-ion batteries," *Energy Environ. Sci.* **5**, 7854 (2012).
- ³N. S. Wade, P. C. Taylor, P. D. Lang, and P. R. Jones, "Evaluating the benefits of an electrical energy storage system in a future smart grid," *Energy Policy* **38**, 7180 (2010).
- ⁴D. P. Finegan, M. Scheel, J. B. Robinson, B. Tjaden, I. Hunt, T. J. Mason, J. Millichamp, M. Di Michiel, G. J. Offer, G. Hinds, D. J. L. Brett, and P. R. Shearing, "In-operando high-speed tomography of lithium-ion batteries during thermal runaway," *Nat. Commun.* **6**, 6924 (2015).
- ⁵X. M. Feng, X. P. Ai, and H. X. Yang, "A positive-temperature-coefficient electrode with thermal cut-off mechanism for use in rechargeable lithium batteries," *Electrochem. Commun.* **6**, 1021 (2004).
- ⁶H. Zhong, C. Kong, H. Zhan, C. Zhan, and Y. Zhou, "Safe positive temperature coefficient composite cathode for lithium ion battery," *J. Power Sources* **216**, 273 (2012).

- ⁷J. Li, J. G. Chen, H. Lu, M. Jia, L. X. Jiang, Y. Q. Lai, and Z. A. Zhang, "A Positive-temperature-coefficient layer based on Ni-mixed poly(vinylidene fluoride) composites for LiFePO₄ electrode," *Int. J. Electrochem. Sci.* **8**, 5223 (2013).
- ⁸P. Arora and Z. M. Zhang, *Chem. Rev.* **104**, 4419 (2004).
- ⁹M. Baginska, B. J. Blaiszik, R. J. Merriman, N. R. Sottos, J. S. Moore, and S. R. White, "Autonomic shutdown of lithium-ion batteries using thermoresponsive microspheres," *Adv. Energy Mater.* **2**, 583 (2012).
- ¹⁰A. V. Le, M. Wang, Y. Shi, D. Noelle, Y. Qiao, and W. Lu, "Effects of additional multiwall carbon nanotubes on impact behaviors of LiNi_{0.5}Mn_{0.3}Co_{0.2}O₂ battery electrodes," *J. Appl. Phys.* **118**, 085312 (2015).
- ¹¹A. V. Le, M. Wang, Y. Shi, D. J. Noelle, and Y. Qiao, "Heat generation of mechanically abused lithium-ion batteries modified by carbon black micro-particulates," *J. Phys. D: Appl. Phys.* **48**, 385501 (2015).
- ¹²M. Wang, A. V. Le, Y. Shi, D. J. Noelle, H. Yoon, M. Zhang, Y. S. Meng, and Y. Qiao, "Effects of angular fillers on thermal runaway of lithium-ion battery," *J. Mater. Sci. Technol.* **32**, 1117 (2016).
- ¹³M. Wang, A. V. Le, D. J. Noelle, Y. Shi, H. Yoon, M. Zhang, Y. S. Meng, and Y. Qiao, "Effects of electrode pattern on thermal runaway of lithium-ion battery," *Int. J. Damage Mech.* (published online).
- ¹⁴Y. Shi, D. J. Noelle, M. Wang, A. V. Le, H. Yoon, M. Zhang, Y. S. Meng, and Y. Qiao, "Exothermic behaviors of mechanically abused lithium-ion batteries with dibenzylamine," *J. Power Sources* **326**, 514 (2016).
- ¹⁵Y. Shi, D. J. Noelle, M. Wang, A. V. Le, H. Yoon, M. Zhang, Y. S. Meng, and Y. Qiao, "Role of amines in thermal-runaway-mitigating lithium-ion battery," *ACS Appl. Mater. Interfaces* **8**, 30956 (2016).
- ¹⁶P. G. Balakrishnan, R. Ramesh, and T. Prem Kumar, "Safety mechanisms in lithium-ion batteries," *J. Power Sources* **155**, 401 (2006).
- ¹⁷E. Kissa, "Wetting and wicking," *Text. Res. J.* **66**, 660 (1996).
- ¹⁸E. W. Washburn, "The dynamics of capillary flow," *Phys. Rev.* **17**, 273 (1921).
- ¹⁹E. Chibowski and L. Holysz, "On the use of washburn's equation for contact angle determination," *J. Adhes. Sci. Technol.* **11**, 1289 (1997).